Ammonia Storage

Ammonia Storage by Reversible Host–Guest Site Exchange in a Robust Metal–Organic Framework

Harry G. W. Godfrey, Ivan da Silva, Lydia Briggs, Joseph H. Carter, Christopher G. Morris, Mathew Savage, Timothy L. Easun, Pascal Manuel, Claire A. Murray, Chiu C. Tang, Mark D. Frogley, Gianfelice Cinque, Sihai Yang,* and Martin Schröder*

Abstract: *MFM-300(Al) shows reversible uptake of NH_3 (15.7 mmol g^{-1} at 273 K and 1.0 bar) over 50 cycles with an exceptional packing density of 0.62 g cm^{-3} at 293 K. In situ neutron powder diffraction and synchrotron FTIR micro-spectroscopy on ND_3@MFM-300(Al) confirms reversible H/D site exchange between the adsorbent and adsorbate, representing a new type of adsorption interaction.*

Approximately 150 million tonnes of NH_3 (ammonia) was produced in 2017, making it one of the most important base chemicals in the world.[1] As an energy resource, NH_3 has an excellent hydrogen density with the hydrogen density of liquid NH_3 and a 200-bar H_2 cylinder being 108 and 14 g L^{-1}, respectively. It also has a high octane number and a low flame temperature, and its combustion to N_2 and H_2O is potentially environmentally benign.[2] As a transportation fuel, NH_3 can be incorporated into existing technologies such as internal combustion engines and gas turbines, but it also holds promise for renewable energy generation through H_2 and NH_3 fuel cells.[2,3] However, under ambient conditions, NH_3 is a toxic and highly corrosive gas making it difficult to handle and store. For it to be transported in an energy efficient manner, NH_3 is often liquefied to maximise its storage density through pipelines and in storage tanks.[4] Liquid NH_3 can be stored at ambient pressure at 240 K, whereas smaller quantities tend to

be stored in pressurised vessels at 16–18 bar.[4a] Reducing or eliminating the energy consumption involved in NH_3 storage is highly desirable, but any prospective material needs to show a high packing density that maximises NH_3 storage amount within a given volume. It also needs to be capable of undergoing multiple cycles whilst retaining its adsorption capabilities. Zeolites, activated carbons, mesoporous silica and organic polymers have been tested for NH_3 storage; however, these materials generally show low and/or irreversible uptakes.[5]

Constructed from metal ions and organic ligands, porous metal–organic frameworks (MOFs) are emerging solid sorbents for a wide variety of substrates.[6] The highly porous nature of MOFs, coupled with their large surface areas (up to 7000 $m^2 g^{-1}$) and high concentration of binding sites, makes them promising candidates for gas storage. Indeed, extensive research efforts have been devoted to studying their capability to serve as H_2, CH_4 and CO_2 stores.[7] However, the potential of utilising MOFs for adsorption of corrosive and toxic gases remain poorly explored,[8] primarily due to the limited stability of many MOFs. Recently, a number of stable MOFs have been tested for NH_3 adsorption with a majority showing structural degradation on exposure or desorption.[9] Here, we examine the adsorption, binding and reversible storage of NH_3 in ultra-stable MFM-300(Al). At 273 K and 1.0 bar, MFM-300(Al) shows an NH_3 uptake of 15.7 mmol g^{-1} {corresponding to a formula of $[Al_2(OH)_2(L)](NH_3)_{6.5}$} leading to a packing density of 0.70 g cm^{-3}, comparable to the liquid density of NH_3 (0.681 g cm^{-3}) at 240 K. At 293 K, MFM-300(Al) also exhibits an impressive packing density of NH_3 at 0.62 g cm^{-3}, higher than leading MOFs and other state-of-the-art porous materials, with an uptake of 13.9 mmol g^{-1}. Importantly, the NH_3 uptake in MFM-300(Al) is fully reversible under conventional pressure-swing conditions, and no loss of storage capacity was observed after 50 cycles of adsorption–desorption at 293 K. We have also employed in situ neutron diffraction, high resolution synchrotron X-ray diffraction and micro-FTIR spectroscopy for determination of the host–guest binding interaction at the molecular level. We have characterised a novel reversible host–guest site exchange mechanism that is intermediate between traditional physisorption and chemisorption.

MFM-300(Al), $[Al_2(OH)_2(L)]$, comprises of $[AlO_4(OH)_2]$ moieties bridged by 3,3′,5,5′-biphenyl-tetracarboxylic acid (H_4L) to afford a rigid "wine-rack" framework with channels of ≈ 6.5 Å in diameter and hydroxyl groups pointing directly into the pore.[10] MFM-300(Al) has demonstrated exceptional adsorption and stability towards corrosive SO_2 and NO_2.[10,11]

[*] H. G. W. Godfrey, L. Briggs, J. H. Carter, Dr. C. G. Morris, Dr. M. Savage, Dr. S. Yang, Prof. M. Schröder
School of Chemistry, University of Manchester
Oxford Road, Manchester, M13 9PL (UK)
E-mail: Sihai.Yang@manchester.ac.uk
M.Schroder@manchester.ac.uk

Dr. I. da Silva, Dr. P. Manuel
ISIS Neutron and Muon Source, Rutherford Appleton Laboratory
Harwell Oxford, Didcot OX11 0QX (UK)

J. H. Carter, Dr. C. G. Morris, Dr. C. A. Murray, Prof. C. C. Tang, Dr. M. D. Frogley, Dr. G. Cinque
Diamond Light Source, Harwell Science and Innovation Campus, Oxfordshire OX11 0DE (UK)

Dr. T. L. Easun
School of Chemistry, Cardiff University
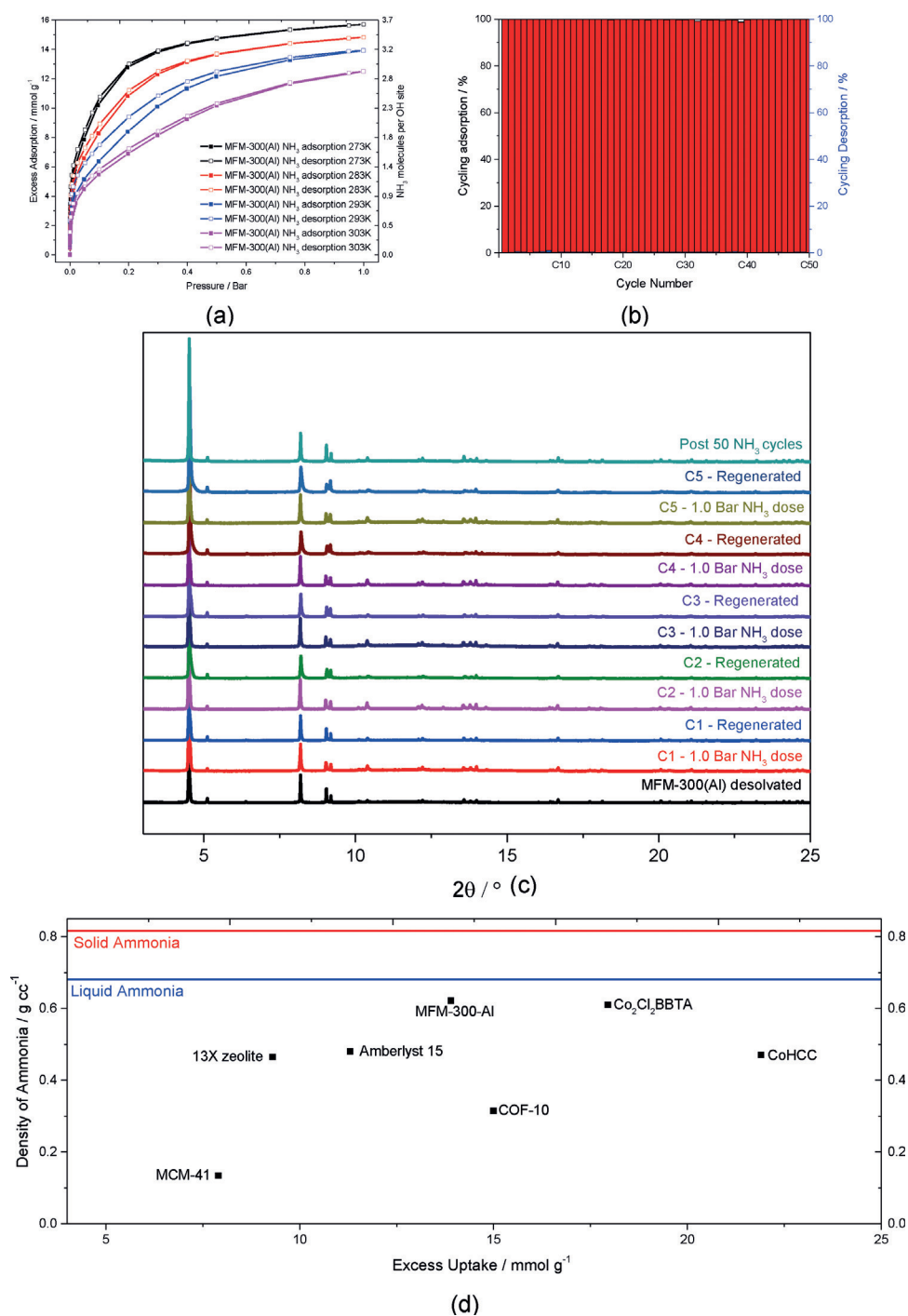Cardiff CF10 3XQ (UK)

(a)

(b)

(c)

(d)

Figure 1. a) Adsorption isotherms of NH₃ in MFM-300(Al) at 273–303 K. b) Repeated cycling of NH₃ up to 50 cycles in MFM-300(Al) at 293 K with percentage adsorption (red) as a function of cycle number and the corresponding desorption (blue) reached for each cycle under pressure-swing conditions. c) PXRD of in MFM-300(Al) cycling with NH₃. d) Comparison of densities of stored NH₃ in MCM-41,[5a] 13X zeolite,[5a] Amberlyst 15,[5a] MFM-300(Al), COF-10,[12] Co₂Cl₂BBTA[9c] and CoHCC[9a] plotted against their respective gravimetric uptake compared with the density of liquid and solid NH₃.

to exposure and suffer significant degradation (Table S7). CoHCC {Co[Co-(CN)₆]₀.₆₀},[9a] [Co₂Cl₂-(BBTA)] [BBTA = 1H,5H-benzo(1,2-d),(4,5-d')bistria-zole)],[9c] COF-10,[12] Amber-lyst 15,[5a] 13X zeolite[5a] and MCM-41[5a] are the best-per-forming porous materials from their respective catego-ries that are stable to repeated NH₃ exposure, with reported uptakes of 21.9 mmol g⁻¹, 18.0 mmol g⁻¹, 15.0 mmol g⁻¹, 11.3 mmol g⁻¹, 9.30 mmol g⁻¹ and 7.90 mmol g⁻¹, respectively, under ambient conditions. MFM-300(Al), while not achieving the highest gravi-metric uptake, supersedes all aforementioned materials in terms of the packing density of NH₃, 0.62 g cm⁻³ at 293 K. Interestingly, MFM-300(Al) can liquefy NH₃ above its boiling point (243 K) by reaching a density of 0.70 g cm⁻³ at 273 K, elimi-nating the need for energy intensive liquefaction for storage.

Significantly, adsorption of NH₃ in MFM-300(Al) is highly reversible with no loss of uptake capacity or crystal-linity, and no broadening of Bragg peaks (Figure S4 in the Supporting Information) was observed after 50 adsorption–desorption cycles at 293 K (Figure 1). CoHCC is able to undergo four cycles with no loss of NH₃ uptake; however, this necessitates reactivation at 150 °C under dynamic vacuum for 24 hrs.[9a] Fur-thermore, each isotherm adsorption point requires 170 minutes for equilibra-tion, thus restricting its potential for portable NH₃

The adsorption isotherms for NH₃ in MFM-300(Al) were measured at 273–303 K, where a total uptake of 15.7 and 13.9 mmol g⁻¹ was recorded at 273 and 293 K, respectively, at 1.0 bar (Figure 1). Due to the reactive nature of NH₃, many materials that have been investigated previously are unstable

storage. [Co₂Cl₂BBTA] and COF-10 both show a loss of NH₃ uptake after repeated cycling of 5.6% and 4.5%, respectively, and for complete regeneration both require heating to 200 °C under dynamic vacuum.[9c,12] In contrast, MFM-300(Al) is able to repeatedly adsorb from regenerated

MOF to complete saturation in 6 mins and completely desorb (saturation to full release) within ≈ 13.5 mins using a standard pressure-swing over 50 cycles, making it an ideal candidate for NH_3 storage.

The binding domains for adsorbed NH_3 molecules within MFM-300(Al) have been elucidated by in situ neutron powder diffraction (NPD). Structural analysis via Rietveld refinement of NPD data for $1.5 ND_3/Al$-loaded MFM-300(Al) identified three distinct binding sites (I, II and III) in $[Al_2(OH)_2(L)](ND_3)_3$ (Figure 2). Site I [occupancy = 0.736-(6)] is 1.76(2) Å {O → N1 = 2.84(1) Å} from the bridging μ_2-OH moiety in a hydrogen bonding pocket formed by the pore wall (Figure 2). The sub 2 Å distance and the high isosteric heat of adsorption ($Q_{st} > 40$ kJ mol^{-1}) are indicative of a strong binding mode being present between NH_3 and MFM-300(Al).[13] Sites II [occupancy = 0.236(3)] and III [occupancy = 0.213(5)] lie at a distance of 2.68(1) Å {N1 → N2 = 3.63(1) Å} and 2.29(3) Å {N2 → N3 = 3.09(1) Å} from site I and site II, respectively. This cooperative network of ND_3 molecules propagates down the length of the 1D channel, anchored in place by site I. Bond distances for sites II···III and a slightly lengthened site I···II are similar to

a typical inter-molecular bond between ND_3 molecules in the solid state at 2 K [N···D = 2.357(2) Å],[14] whereas the bond between the framework μ_2-OH and site I is significantly shorter. The structure for ND_3-loaded MFM-300(Al) has also been determined at a loading of $0.5 ND_3/Al$ and $1.0 ND_3/Al$ and these have shown similar binding sites as discussed above. With increased loading from $0.5 ND_3/Al$ to $1.5 ND_3/Al$, we observed an overall shortening of the framework μ_2-OH···site I and sites I···II and an increase in the site II···III.

Refinement of the NPD data for ND_3-loaded MFM-300(Al) revealed an interesting observation: as the loading of ND_3/μ_2-OH was increased, the hydrogen on hydroxyl groups underwent a reversible site exchange with the deuterium from guest ND_3 molecules residing at Site I in the pore. This exchange is very distinct in the analysis of NPD data owing to the significant difference on neutron scattering of hydrogen and deuterium. We noted as the loading of ND_3 increased from 0 to $0.5 ND_3/\mu_2$-OH, the occupancy of the hydrogen of the μ_2-OH group decreased from 1.0 to 0.794(7) (Table S6). As the loading of ND_3 was further increased to 1.0 and $1.5 ND_3/\mu_2$-OH, the occupancy of the hydrogen on the μ_2-OH group decreased to 0.416(10) and the site was replaced by a deuterium to give a μ_2-OD [D occupancy = 0.468(9) and 0.584(10), respectively].

We sought to examine the reversibility of this H–D exchange via in situ synchrotron FTIR micro-spectroscopy by monitoring the νO-H stretching vibration at 3692 cm^{-1} as a function of ND_3 loading at 293 K (Figure 3). A rapid depletion of this band was observed on adsorption of ND_3 under flow conditions, accompanied by the growth of a new band at 2720 cm^{-1} assigned to the νO-D stretching mode, thus confirming H→D exchange. Once the H→D exchange is completed to give $[Al_2(OD)_2(L)]$ with no residual O-H stretching band observed, the material was charged with a flow of NH_3 at 293 K. Interestingly, the νO-D stretching
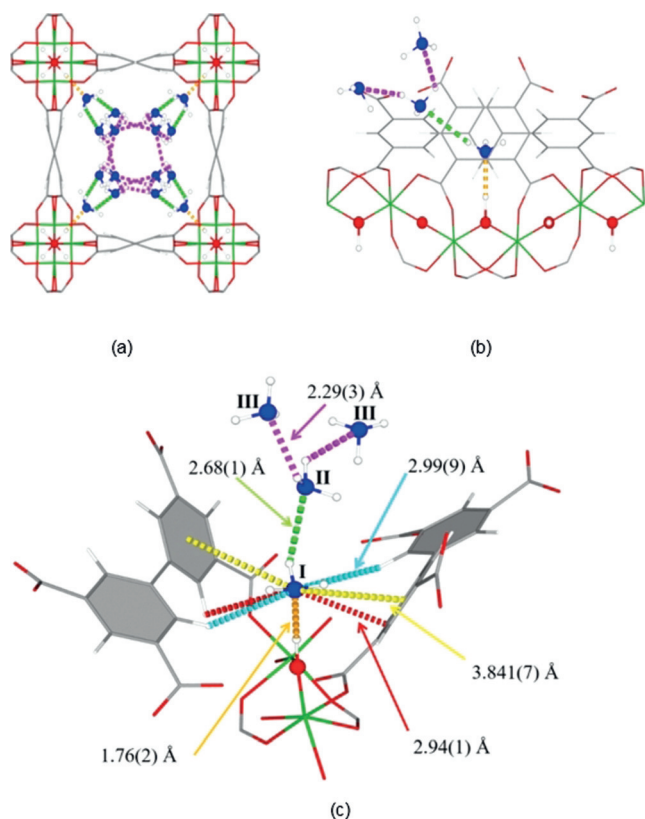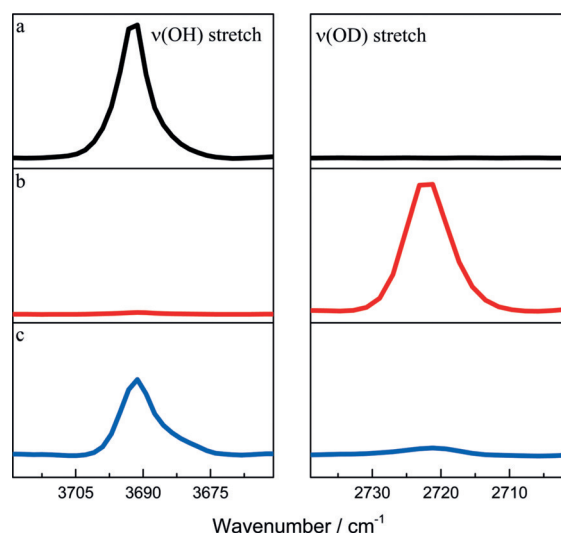
Figure 2. View of the structure of $1.5 ND_3/Al$-loaded MFM-300(Al) determined by in situ NPD studies. a) View down the c-axis; b) side on view of three binding sites in relation to the OH functionality; c) view of binding of ND_3 to the framework. Framework hydrogen → Site I (orange) = 1.76(2) Å {O → N1 = 2.84(1) Å}. Linker ring → Site I (yellow) = 3.841(7) Å. Linker H1 → Site I (red) = 2.94(1) Å. Linker H2 → Site I (indigo) = 2.994(9) Å. Site I → Site II (green) = 2.68(1) Å {N1 → N2 = 3.63(1) Å}. Site II → Site III (purple) = 2.29(3) Å {N2 → N3 = 3.09(1) Å}.

Figure 3. Reversible switching of framework hydroxyl hydrogen from H→D→H. The ν(OH) stretching vibration is at 3692 cm^{-1} and the ν(OD) stretching vibration at 2720 cm^{-1}. a) Bare MFM-300(Al) (black); b) ND_3 exposed MFM-300(Al) (red) and c) regenerated hydroxyl H functionalised MFM-300(Al) after exposure of (b) to NH_3 (blue).

band at $2720\,cm^{-1}$ disappeared and the νO-H band at $3692\,cm^{-1}$ returned, indicating that the H→D exchange is completely reversible. It is worth noting that such H–D reversible exchange does not lead to any detectable structural degradation of the long range order of the framework (Figure S8). Traditionally, chemisorption and physisorption is distinguished on the basis of host–guest binding interaction and the formation of adsorbate–adsorbent bonds at the interface. Significantly, the adsorption of ND_3 in MFM-300(Al) revealed a new type of adsorption where adsorbent and adsorbates undergo rapid site-exchange via reversible formation and cleavage of O−H and O−D chemical bonds.

In summary, MFM-300(Al) shows excellent NH_3 adsorption capacity with the intrinsic ability to achieve liquefaction of NH_3 under near ambient conditions, and outperforms the state-of-the-art porous materials in terms of NH_3 packing density, reversibility and stability. MFM-300(Al) offers unparalleled repeatable uptake characteristics and, coupled with the pseudo-chemisorption binding mechanism, is a promising NH_3 storage material for portable applications.

CCDC 1856081, 1856082, 1856083 and 1856084 contain the supplementary crystallographic data for this paper. These data can be obtained free of charge from The Cambridge Crystallographic Data Centre. Correspondence and requests for materials should be addressed to S.Y. (Sihai.Yang@manchester.ac.uk) and M.S. (M.Schroder@manchester.ac.uk).

Conflict of interest

The authors declare no conflict of interest.

[1] J. A. Ober, *Mineral Commodity Summaries*, Reston, VA, **2018**, p. 204.

[2] A. Klerke, C. H. Christensen, J. K. Nørskov, T. Vegge, *J. Mater. Chem.* **2008**, *18*, 2304–2310.

[3] a) F. R. Westlye, A. Ivarsson, J. Schramm, *Fuel* **2013**, *111*, 239–247; b) D. R. Jenkins, *Hypersonics before the shuttle: A concise history of the X-15 research airplane*, NASA, **2000**; c) F. Schüth, R. Palkovits, R. Schlögl, D. S. Su, *Energy Environ. Sci.* **2012**, *5*, 6278–6289; d) R. Lan, J. T. S. Irvine, S. Tao, *Int. J. Hydrogen Energy* **2012**, *37*, 1482–1494; e) T. Per, H. Christian, A. Serina, *Environ. Prog. Sustainable Energy* **2014**, *33*, 1290–1297.

[4] a) "Ammonia, 1. Introduction": M. Appl in *Ullmann's Encyclopedia of Industrial Chemistry*, Wiley, Hoboken, **2011**; b) G. Thomas, *Potential roles of ammonia in a hydrogen economy*, U.S. Department of Energy, **2006**.

[5] a) J. Helminen, J. Helenius, E. Paatero, I. Turunen, *J. Chem. Eng. Data* **2001**, *46*, 391–399; b) J. F. Van Humbeck, T. M. McDonald, X. Jing, B. M. Wiers, G. Zhu, J. R. Long, *J. Am. Chem. Soc.* **2014**, *136*, 2432–2440.

[6] S. Kitagawa, *Chem. Soc. Rev.* **2014**, *43*, 5415–5418.

[7] a) Y. He, W. Zhou, G. Qian, B. Chen, *Chem. Soc. Rev.* **2014**, *43*, 5657–5678; b) L. J. Murray, M. Dincă, J. R. Long, *Chem. Soc. Rev.* **2009**, *38*, 1294–1314; c) K. Sumida, D. L. Rogow, J. A. Mason, T. M. McDonald, E. D. Bloch, Z. R. Herm, T. H. Bae, J. R. Long, *Chem. Rev.* **2012**, *112*, 724–781.

[8] E. Barea, C. Montoro, J. A. Navarro, *Chem. Soc. Rev.* **2014**, *43*, 5419–5430.

[9] a) A. Takahashi, H. Tanaka, D. Parajuli, T. Nakamura, K. Minami, Y. Sugiyama, Y. Hakuta, S. Ohkoshi, T. Kawamoto, *J. Am. Chem. Soc.* **2016**, *138*, 6376–6379; b) A. J. Rieth, Y. Tulchinsky, M. Dincă, *J. Am. Chem. Soc.* **2016**, *138*, 9401–9404; c) A. J. Rieth, M. Dincă, *J. Am. Chem. Soc.* **2018**, *140*, 3461–3466.

[10] a) S. Yang, J. Sun, A. J. Ramirez-Cuesta, S. K. Callear, W. I. David, D. P. Anderson, R. Newby, A. J. Blake, J. E. Parker, C. C. Tang, M. Schröder, *Nat. Chem.* **2012**, *4*, 887–894; b) S. Yang, A. J. Ramirez-Cuesta, R. Newby, V. Garcia-Sakai, P. Manuel, S. K. Callear, S. I. Campbell, C. C. Tang, M. Schroder, *Nat. Chem.* **2015**, *8*, 121–129; c) X. Han, H. G. W. Godfrey, L. Briggs, A. J. Davies, Y. Cheng, L. L. Daemen, A. M. Sheveleva, F. Tuna, E. J. L. McInnes, J. Sun, C. Drathen, M. W. George, A. J. Ramirez-Cuesta, K. M. Thomas, S. Yang, M. Schröder, *Nat. Mater.* **2018**, *17*, 691–696.

[11] M. Savage, Y. Cheng, T. L. Easun, J. E. Eyley, S. P. Argent, M. R. Warren, W. Lewis, C. Murray, C. C. Tang, M. D. Frogley, G. Cinque, J. Sun, S. Rudić, R. T. Murden, M. J. Benham, A. N. Fitch, A. J. Blake, A. J. Ramirez-Cuesta, S. Yang, M. Schröder, *Adv. Mater.* **2016**, *28*, 8705–8711.

[12] C. J. Doonan, D. J. Tranchemontagne, T. G. Glover, J. R. Hunt, O. M. Yaghi, *Nat. Chem.* **2010**, *2*, 235–238.

[13] a) G. A. Jeffrey, G. A. Jeffrey, *An introduction to hydrogen bonding*, Vol. 12, Oxford University Press, New York, **1997**; b) G. R. Desiraju, T. Steiner, *The weak hydrogen bond: in structural chemistry and biology*, Vol. 9, International Union of Crystallography, **2001**.

[14] A. W. Hewat, C. Riekel, *Acta Crystallogr. Sect. A* **1979**, *35*, 569–571.